Top Catal (2018) 61:299–307
DOI 10.1007/s11244-017-0855-4

ORIGINAL PAPER

# Structural Differentiation of the Reactivity of Alcohols with Active Oxygen on Au(110)

**Fanny Hiebel[1] · Stavros Karakalos[1,3] · Yunfei Xu[1] · Cynthia M. Friend[1,2] · Robert J. Madix[2]**

Published online: 25 September 2017


**Abstract** A wide range of oxidative coupling reactions occur under mild conditions on gold, all of which are activated by atomically adsorbed oxygen ($O_{ads}$). We have examined the reactivity of methanol and ethanol for self-coupling with well-ordered O-covered Au(110) surface structures, characterized by scanning tunneling microscopy (STM). Zig-zag O chains along the reconstructed (1 × 2) surface are observed up to a coverage of 0.25 Ml O that evolve into double row structures filling all threefold hollow sites along the topmost rows of gold atoms up to 0.5 Ml. Surface roughening occurs above 0.5 Ml O. Below 0.08 Ml O, both alcohols exhibit 100% selectivity for self-coupling to their corresponding ester. This adsorbed O consumed by abstraction of the alcoholic hydrogen, to form the adsorbed alkoxide. Under these conditions further C–H bond of both the adsorbed alkoxy and hemiacetal alcoholate intermediates necessary to form the ester predominates over reactions assisted by $O_{ads}$. Above ~0.08 Ml the alcohols react very differently. Methanol is not activated by additional adsorbed O, whereas ethanol reacts readily up to a coverage of 0.35 Ml O. We attribute this differentiation to both a change in the energetics of the O bonding to the surface and differences in the energetics of reaction of the two alcohols to form adsorbed alkoxides.

**Keywords** Au(110) · Alcohols · Gold catalysis · Selective oxidation · Structure sensitivity

## 1 Introduction

The binding state of atomic oxygen to metal surfaces is clearly of fundamental importance to the kinetics and mechanism of catalytic oxidation processes. Understanding the relationship between the state of oxygen binding and its reactivity towards reducing gases, including the effect of 2-D order, is therefore essential [1–7]. For example, it has been shown that on Au(111) adsorbed O dispersed at low coverage reacts readily with CO, whereas at higher coverage a 2D oxide forms that is much less reactive [8]. Also, adsorbed atomic O reacts anisotropically with CO and $CH_3OH$ on Cu(110) due to its propensity to form condensed island structures [9]. In particular, both CO and $CH_3OH$ react preferentially with O at the end of the chains that comprise the islands rather than from the sides [6, 10]. In contrast, formic acid reacts spatially homogeneously with O in the Cu(110)-(2 × 1)O structure [11]. On Ag(110) metal-O chains also form along the (110) direction; however in this case the added rows repel one another and easily fragment into short segments at low O coverages which readily react [12–14]. Thermal fluctuations in the chain lengths thus sufficiently destabilize the chains so that active sites for CO oxidation are introduced at the ends of the short chains at relatively low temperature [15]. For more complex reactions, such as

Fanny Hiebel and Stavros Karakalos are Co-First Authors.

**Electronic supplementary material** The online version of this article (doi:10.1007/s11244-017-0855-4) contains supplementary material, which is available to authorized users.

✉ Robert J. Madix
rmadix@seas.harvard.edu

[1] Department of Chemistry and Chemical Biology, Harvard University, Cambridge, MA, USA

[2] School of Engineering and Applied Science, Harvard University, Cambridge, MA, USA

[3] Present Address: Department of Chemical Engineering, Swearingen Engineering Center, University of South Carolina, Columbia, SC 29208, USA

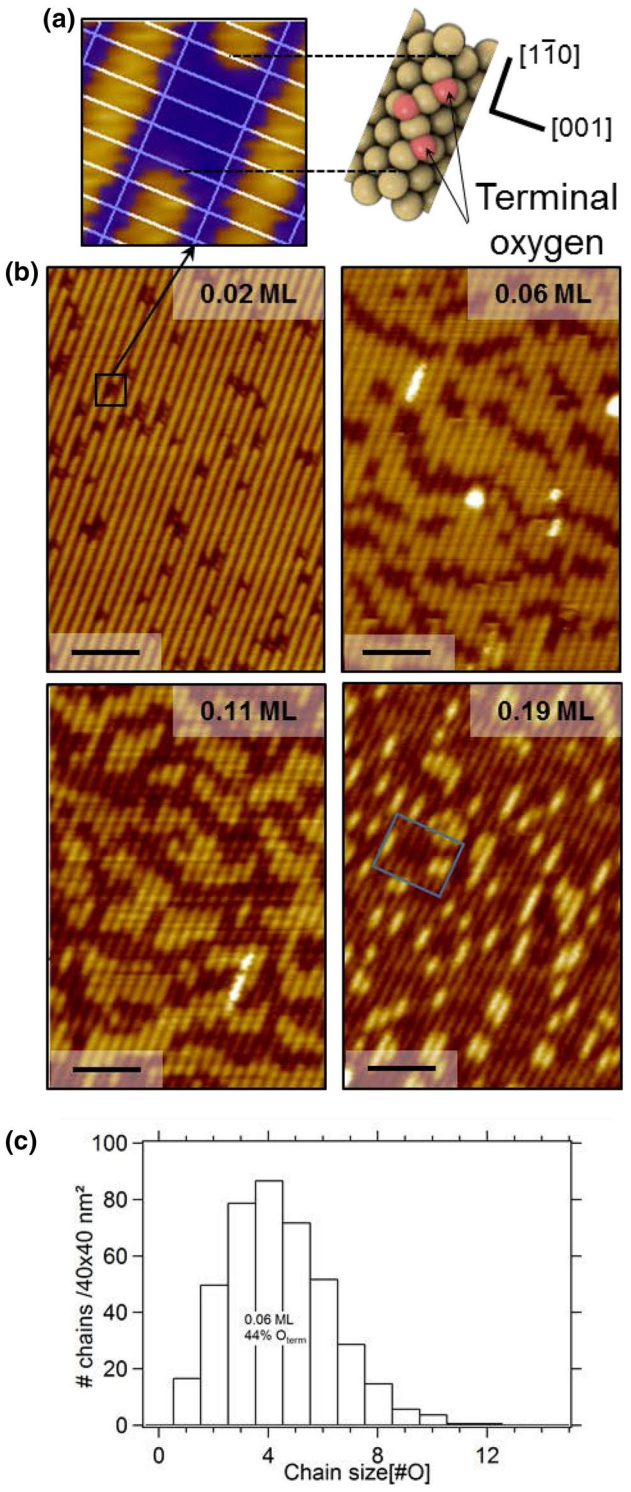


**Fig. 1** O ordering as a function of O coverage, below 0.25 Ml. **a** ▶ A 3-O chain images as four aligned dark cells due to the tunneling conditions. Each chain contains two terminal O atoms. Imaging parameters: (+ 1.5 V, 0.2 nA), the grid represents the 2.88×8.16 Å$^2$ Au(110)-(1×2) surface lattice. **b** Series of STM images of increasing total O coverage showing the ordering of the O chains (dark amber) into islands across the Au rows. At 0.19 Ml coverage, darker stripes are observed across the rows (see boxed area). Scale bar: 5.0 nm. **c** Histogram of the chain lengths measured on the surface with 0.06 Ml of O in (**b**) over a 40×40 nm$^2$ surface. Terminal O represent 44% of the adsorbed O (corresponding to ~0.03 Ml)

alcohol coupling over gold catalysts [16], such structural sensitivities may be of importance in determining reaction selectivities. Herein, we report that the ordering of O on Au(110) affects the reactivity with methanol and ethanol in significantly different ways.

The reactivity was examined at atomic length scales using a combination of scanning tunneling microscopy and temperature programmed reaction. Previous work demonstrated that oxygen atoms occupy pseudo threefold sites along the facets of the (1×2) reconstruction of the Au(110) at all coverages up to 0.5 Ml; however, the longer range order of the O depends on coverage [17]. At extremely low coverage (<0.08 Ml), the oxygen atoms are highly dispersed, forming isolated O atoms and short (~3 atom) chains. As the coverage increases, the O forms zig-zag chains up to a coverage of 0.25 Ml (Fig. 1a). In this regime longer chains and 2-D islands form, all with the zig-zag structure (Fig. 1b). Ab initio calculations also indicate that O is stabilized as a result of this chain-like structures [17, 18].

As shown herein, above a coverage of 0.25 Ml O double-row symmetric chains form up to a saturation of 0.5 Ml. Notably, there is no strong restructuring of the Au atoms upon adsorption in this regime; the basic (1×2) reconstruction is maintained. Above 0.5 Ml of O, metal atoms are expelled from the surface and a complex, ill-defined structure forms. One Ml is defined using all the exposed Au atoms in the native missing row reconstruction, including those in the (111) microfacets, i.e. four atoms per Au(110)-(1×2) unit cell (Fig. S1) [17].

Herein the interplay between the degree of ordering of adsorbed O and the length of the alkyl group of methanol and ethanol, respectively, was investigated. The reactivity of methanol and ethanol towards O on Au is of interest, because a range of highly selective oxidative coupling reactions of alcohols to esters is achievable on O-activated Au under mild conditions at low O coverages [19]. The first reaction step in these complex reactions is the deprotonation of the alcohol by adsorbed atomic O and formation of an alkoxy and hydroxyl on the surface; the OH further reacts with additional alcohol to yield $H_2O$ (Scheme 1) [20]. At low oxygen coverages dehydrogenation of the alkoxy produces the aldehyde, which either desorbs or couples with other alkoxy species to yield an ester (Scheme 1) [21, 22]; secondary alcohols exclusively yield ketones [23, 24]. At higher O coverages, secondary combustion of reaction intermediates or the products may also occur with residual adsorbed oxygen. It could be deduced that the loss of selectivity from coupling to combustion is the result of increased

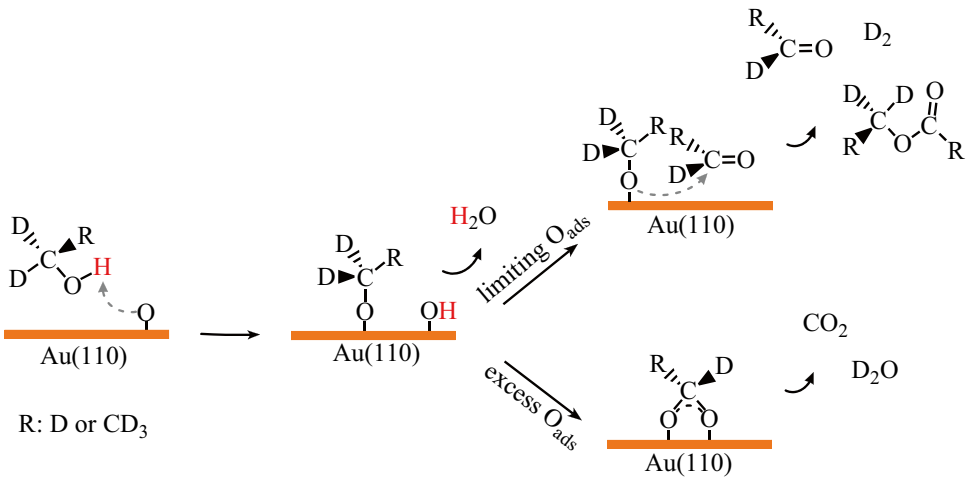


**Scheme 1** Mechanism of isotopic labeled methanol and ethanol oxidation reactions on O/Au(110)

local O concentration. Therefore it is important to understand the patterns of reactivity of alcohols with adsorbed O, especially in the context of O ordering, which is governed by the O coverage.

We observed significant variation in reactivity and selectivity for both methanol and ethanol, as a function of the oxygen ordering on the surface. Both alcohols react facilely and selectively at low O coverage where the adsorbed oxygen is highly dispersed, suggesting that single O atoms or O at the chain ends of the zig-zag structure is most reactive. At higher coverages, where longer chains form and condense into 2D islands, reactivity is diminished. The maximum amount of methanol reaction occurs at 0.08 Ml of O, and methyl formate is the main product from reaction, formed by reaction with a single adsorbed O. Above this O coverage islands comprised of collections of longer O chains are present with a smaller percentage of chain ends, and no further conversion of methanol is observed. On the other hand, ethanol selectively reacts at coverages up to 0.35 Ml of O, a distinct transition being observed at 0.10 Ml O whereby additional adsorbed O contributes to ethyl acetate formation via activation of C–H bonds in the reaction intermediates. Secondary reactions occur at higher O coverage. This clear demarcation in the reactivity of the two alcohols is surprising and has not been previously observed.

## 2 Experimental

The Au(110) single crystal was purchased from Princeton Scientific. Cleaning cycles of sputtering and annealing at ~900 K were performed until no impurity trace was detected by Auger electron spectroscopy, and STM showed a uniform Au(110)(1 × 2) surface. Atomic O was adsorbed on the surface upon room temperature ozone exposure, following the procedure described elsewhere [17]. Prior to STM experiments, the samples were mildly annealed to ~450 K for 5 min, although we observed that annealing did not dramatically impact the O structures. STM experiments were conducted under base pressure below $1.0 \times 10^{-10}$ mbar using an Omicron VT-STM and mechanically cut Pt-Ir tips. Typical scanning rate was 300–500 nm/s, bias voltage + 1.5 V and low tunneling current of 0.1–0.2 nA. Imaging was performed at a low temperature of 150–170 K and room temperature. Some O movement was observed at room temperature, which was quenched at low temperature. O counts were performed using the SPIP image processing software, based on the number of dark chains and their length distribution (in the row direction).

Temperature programmed reaction spectroscopy experiments were performed on a Au(110) single-crystal in a separate UHV chamber with a base pressure $<5 \times 10^{-10}$ Torr. The Au(110) crystal was mounted on a manipulator capable of heating to 1000 K and of cooling (via liquid nitrogen) to 100 K, as measured by a chromel–alumel thermocouple inserted into a pinhole in the side of the Au(110) crystal. The Au(110) was cleaned by argon ion bombardment followed by cycles of ozone dosing at 200 K and flash annealing to 850 K to remove surface impurities (as judged by CO and $CO_2$ production from C contamination). Surface cleanliness was confirmed by recording the ordered (1 × 2) reconstruction LEED pattern of Au(110) surface. Adsorbed atomic oxygen was generated by controlled dosing of ozone to the surface, and the coverage was calibrated by comparison of the intensity of the integrated $O_2$ signal due to O atomic recombination above 500 K to the integrated signal for the saturation coverage of 1 Ml. A detailed description of the O calibration is in the supplementary information (Fig. S2).

Mass spectrometry was used to quantify the concentrations of products on the surface. The coverages were calibrated by comparison of the intensity of the integrated peak signal obtained during temperature programmed reaction, due to the product desorption to the integrated signal for the saturation coverage of 1 Ml of $O_2$, after correction of the

peak intensities. The correction was performed taking into account the differences in fragmentation pattern, transmission coefficient, detection coefficient and ionization cross-section of the masses detected (Tables S1 and S2).

Reactants were introduced to the catalyst surface at the temperatures specified (~130 K), using directed dosers and monitoring the rise in the ambient pressure in the chamber while leaking the respective vapor into the UHV system. The fragmentation patterns of the background gas, recorded from condensation experiments on Au(110), verified the gas purity. Methanol was subjected to several freeze–pump–thaw cycles for purification before use. A typical experiment consisted of ozone exposure to the catalyst surface at 300 K followed by cooling of the sample to ~130 K before dosing methanol. The catalyst was then heated and the reaction monitored by TPRS (Figs. S3, S4). The heating rate for temperature programmed reactions was constant at ~5 K $s^{-1}$. The reaction products were identified by quantitative mass spectrometry (Hiden HAL/3F) using fragmentation patterns obtained from authentic samples (See Supplemental Information, section III).

## 3 Results

### 3.1 Coverage Dependent Oxygen Ordering

As shown previously O is bound in pseudo-3 fold sites of the reconstructed Au(110)-(1 × 2) surface without reversal of the clean surface (1 × 2) reconstruction. Zig-zag ordering of O is observed at coverages ranging from 0.02 to 0.19 Ml (Fig. 1). Under the tunneling conditions employed, n-contiguous O atoms in the zig-zag arrangement image as a dark feature (n + 1) Au atoms long, along the ridges in the (1 × 2) reconstruction. Mild annealing (~450 K for 5 min) does not affect the surface structure observably. At very low coverage O-atoms are highly dispersed; however even at coverage as low as 0.02 Ml pairing of atoms is observed. Already at a coverage of 0.06 Ml, O chains with a distribution of chain length coalesce into structures running perpendicular to the close-packed Au rows (Fig. 1c); their length is limited along the rows. Both the limitation in chain length and the islanding of the chains result from strain induced in the Au surface upon O adsorption [17]. A similar structural pattern is maintained at 0.11 Ml, with two-dimensional islands of the chains separated by ~4 nm along the $(1\bar{1}0)$ direction (the close-packed direction of the underlying Au rows). At 0.19 Ml the surface is close to being saturated with the O chains—an ideal completed zig-zag layer corresponding to 0.25 Ml of O. Darker linear features are observed (see boxed area), although their exact nature is unknown. Those defects are distributed on the surface in a way that also suggests that they arise to release strain from the O adsorption.

At higher coverage a stable adsorption configuration with local coverage of 0.5 Ml in the form of a symmetric chain is observed that was proposed previously from DFT calculations (Fig. 2b, c) [18]. The dark stripes observed along the rows at 0.4 Ml (particularly in the annealed experiment) show evidence of those symmetric chains. Bright features are ~0.5 Å high and thus are taken to correspond

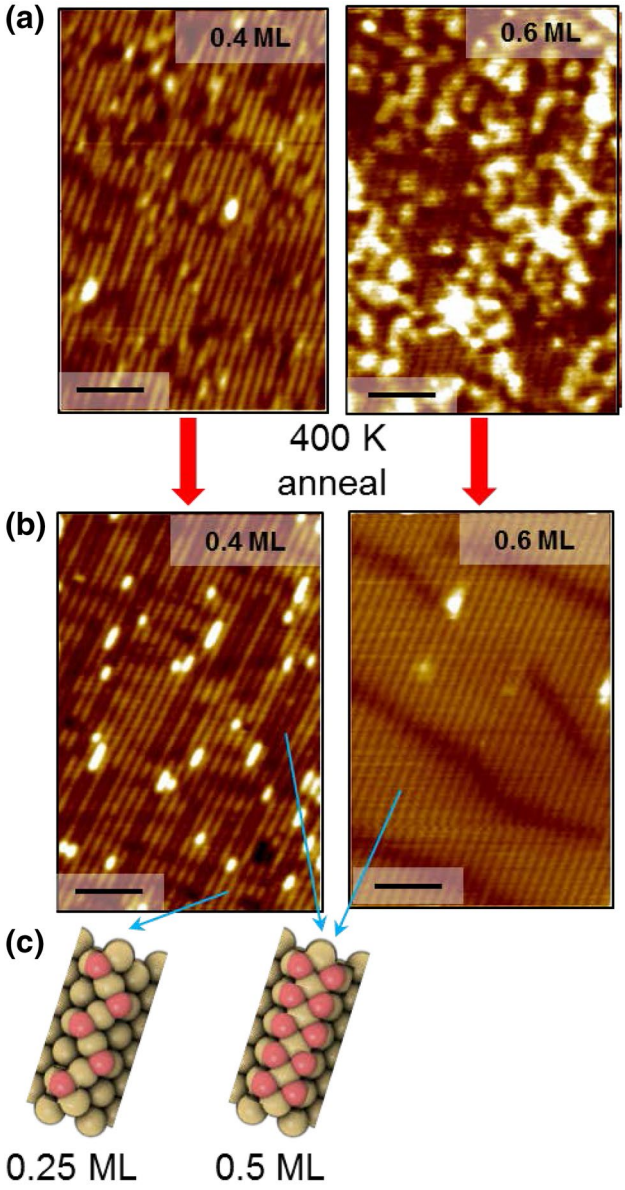


**Fig. 2** O ordering as a function of O coverage above 0.25 Ml. **a** Surface as deposited showing the onset of surface roughening ~0.5 Ml. **b** Annealed surface showing smooth, ordered structures, in particular dark linear structures along the rows at 0.4 Ml and across the rows at 0.6 Ml. **c** Proposed ordered local O adsorption structures and their corresponding local coverages. STM images in (**a**) and (**b**) were conducted at room temperature. Imaging parameters were 300–500 nm/s for the scanning rate, + 1.5 V for the bias voltage, and + 0.2 nA for the tunneling current. Scale bar: 5.0 nm

to remaining clean Au areas. Chains of similar geometry have been observed on Rh(110), [25, 26]. although the missing row reconstruction is induced upon adsorption of O. On Rh(110) the O atoms within chains can have different reactivity towards adsorbed H atoms, due to strain induced in the surface [27]. On Au(110), there is no reversal in the reconstruction of the clean Au(110)-(1×2) structure and no incorporation of metal atoms into the adsorbate structure below 0.5 Ml O, in contrast to what is observed on Cu(110) and Ag(110) [9, 14, 28].

At yet higher coverage O adsorption induces disorder, and at 0.6 Ml significant restructuring occurs, indicated by the large bright features on the surface that are ascribed to rearrangement of the Au (Fig. 2a). Upon annealing to 400 K this disordered surface is transformed to a smooth (1×2) with some 1D patterning perpendicular to the rows (dark features). We interpret the structure above 0.25 Ml as being covered with symmetric O chains and defective areas (darker features) which release strain (Fig. 2c). Of course, these symmetric, double row configurations may begin to develop below 0.25 Ml O as the zig-zag structures begin to saturate. There is no evidence for subsurface O using temperature programmed desorption, independent of pre-annealing treatment (not shown). We have insufficient information for a detailed interpretation of the higher coverage, reconstructed structures.

### 3.2 Reactivity of Methanol and Ethanol

At low initial O coverage, up to ~0.08 Ml, both methanol and ethanol selectively form methyl formate and ethyl acetate, respectively. These are the only products detected other than water, hydrogen and the alcohol itself, indicating ~100% selectivity for ester formation (Figs. 3, S3). Quantitative analysis of the product yields shows that one ester is formed per O initially adsorbed in this coverage regime (Figs. 3, 4, S3–S6). Details regarding the quantitative analysis are provided in the Supplementary Information (Tables S1, S2; Figs. S5, S6).

The selective oxidation of alcohols on Au is known to result from the formation of their corresponding adsorbed alkoxy species by extraction of the hydroxyl hydrogen by the adsorbed O (Scheme 1) [29]. This initiation step is confirmed by the fact that $H_2O$ is evolved at the temperature

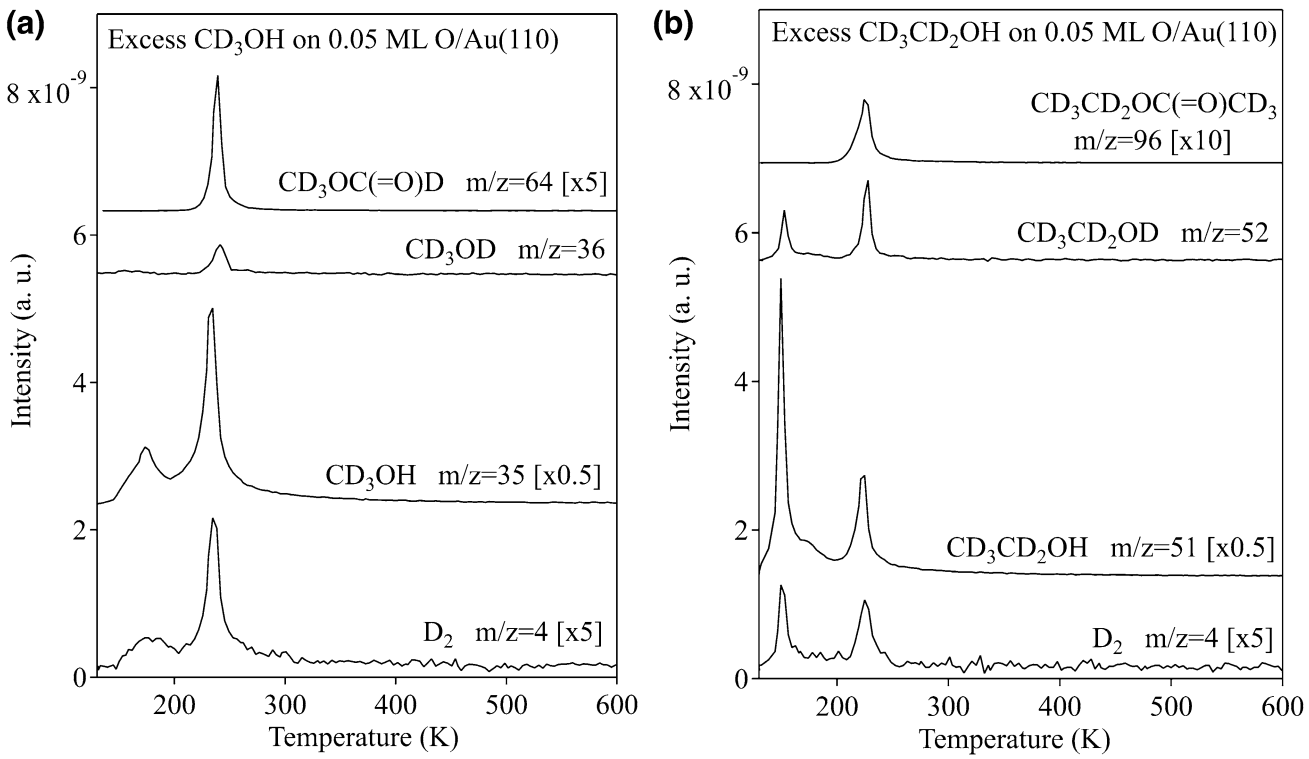


**Fig. 3** Temperature programmed reaction spectroscopy of: **a** $CD_3OH$ and **b** $CD_3CD_2OH$ for low initial O coverage (0.05 Ml). The data has been corrected for fragmentation (See SI). The only products detected are those shown as well as isotopes of water and other isotopes of hydrogen (See Fig. S2). Note the coincident production of $D_2$ and the deuterated alcohol with desorption of the ester. All data were obtained after exposure of excess alcohol to a surface precovered with a known amount of O at 130 K. The heating rate was 5 K/s in all cases. The isotopic purity of the $CD_3OH$ is 0.96 and 0.95 for $CD_3CD_2OH$ based on measurement of parent peak intensities for the perhydrido- and perdeutero-alcohols condensed on clean Au(110)-(1×2)

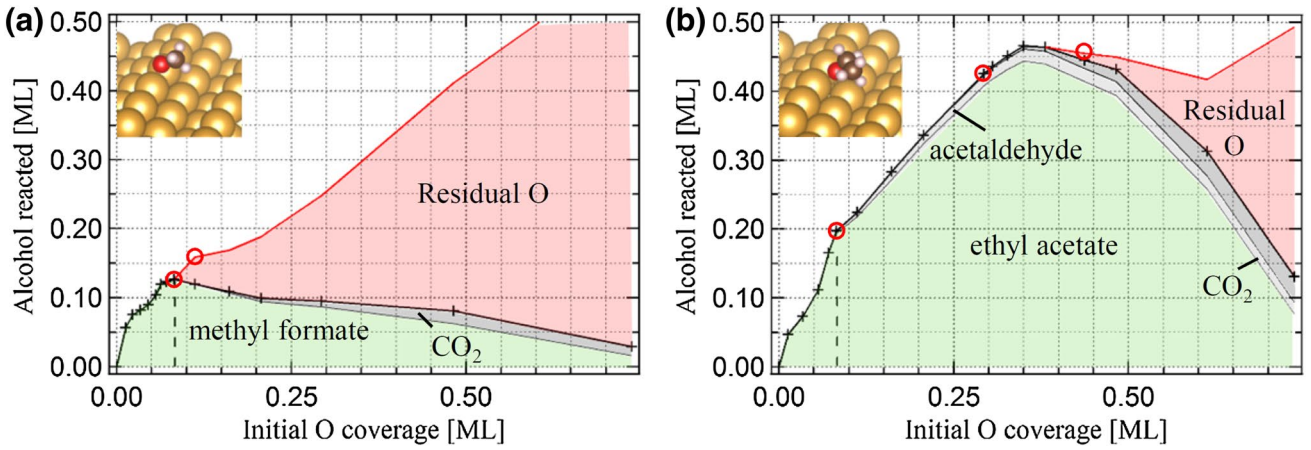


**Fig. 4** Amount of alcohol reacted (bold line) and the relative products (shaded areas) and residual O (red) as a function of initial O. **a** Methanol oxidation. **b** Ethanol oxidation. More exact details of the dependence of product yields on O precoverage are shown in Figs. S5, S6. Inset: adsorption geometry of the respective alkoxy [34]

for water desorption from Au(110), from reaction of both $CD_3OH$ and $CD_3CD_2OH$ (~170 K) (Fig. S3). Little or no $D_2O$ or HDO was detected (Fig. S3). Furthermore, no reaction was observed if the alcohols were condensed on clean Au(110)-(1 × 2) (data not shown) [30, 31].

Based on the predominance of $D_2$ formed from both conversion of $CD_3OH$ and $CD_3CD_2OH$ to their corresponding esters, the initially adsorbed O is utilized to form the alkoxide, and the ensuing β-CH(D) activation to form the aldehyde, is induced by neighboring Au atoms at low initial O coverage (Fig. 3, S3, S4, S5, and S6). Analysis of the temperature programmed reaction data obtained for excess alcohol and very low O coverage, reveals 100% selectivity to the ester and prominent $D_2$ and $CD_3OD$ signals coincident with the ester desorption for both species (Fig. 3 and S3). This observation clearly indicates the release of D atoms to the surface upon dehydrogenation of the alkoxide. Furthermore, surface O is also not required for the ensuing abstraction of the additional D atom from the hemiacetal alcoholate intermediate, formed from coupling of an aldehyde and alkoxide on the surface (Scheme 1) [32, 33]. At these low O coverages the $O_{ads}$ is preferentially consumed by reaction with the alcohol to form the alkoxy, forcing the β-D abstraction to occur via Au insertion into the C–D bond. The activation of the C–H bond by the gold surface is an important observation, given the relative inertness of Au surfaces.

The dependence of the yield of ester on the initial $O_{ads}$ coverage and structure reveals important differences in the reactivity of methanol and ethanol. At higher initial O coverage, the selectivity decreases and the ratio of the ester formed to the initial O coverage decreases for both methanol and ethanol (Fig. 4, S5, and S6). In the case of methanol, the amount of methyl formate formed from methanol diminishes and some $CO_2$ is formed for initial O coverages above 0.08 Ml (Fig. 4, S4–S6). As the initial O coverage is increased, there is also a gradual decrease in overall reactivity such that there is little or no methanol conversion at an initial O coverage of 0.75 Ml. Furthermore, not all O reacts with the methanol, leading to recombination and desorption of excess oxygen as $O_2$ above 500 K and formation of some $CO_2$ (Fig. 4, S4–S6). The decrease in methanol reactivity and selectivity corresponds to the more densely packed O structure.

While the key features of methanol and ethanol oxidative coupling at low O coverage are essentially the same, their reactivity differs at higher O coverage where more densely packed O structures are present. Up to an initial coverage of O of ~0.08 Ml—conditions where the O atoms are highly dispersed—the selectivity for ester formation from both methanol and ethanol is 100% and all adsorbed O is consumed (Figs. 4, S4–S6). Quantitative analysis of the temperature programmed reaction data shows that there is a 2:1 ratio of the amount of alcohol that reacts per initial O coverage in this regime (one ester per adsorbed O). The selectivity and stoichiometry of the coupling reaction were quantified by assuming that consumption of the adsorbed O at low coverage was due to the removal of the hydroxyl hydrogen, thus yielding one molecule of ester per preadsorbed O at the lowest O coverages, as described in the supplementary information. This assumption was verified by the quantitative mass spectrum analysis of the relative amounts of methyl formate formed per O adsorbed for methanol. A more detailed plot and fit of the data, as well as the quantitative analysis of the amount of methyl formate formed is shown in Figs. S5–S7.

At higher initial O coverages (~0.35 Ml) the ethanol reactivity decreases, indicating its reactivity is less with the more densely packed O structures. The ratio of ester formed-to-O consumed changes to a ratio of 1:2 ester between 0.08 and

0.35 Ml O (Figs. 4, S6). Furthermore, in this range of O coverage, all oxygen continues to be consumed by reaction with ethanol. A small amount of acetaldehyde is observed from the reaction of ethanol in this coverage range as well, whereas no formaldehyde was detected for methanol under any conditions. The abrupt change in stoichiometry of the reaction of ethanol with preadsorbed O to 1:2 from 1:1 above 0.08 Ml of O indicates that the adsorbed O promotes β-C–D(H) scission in the secondary steps in the mechanism of ethylacetate formation at the higher O coverages, most likely by reaction with the ethoxy, since that is the second dehydrogenation step in the reaction sequence to form the ester.

At O coverages greater than 0.35 Ml—a regime where the double row structure begins to predominate and saturates near 0.5 Ml—the amount of ethanol reaction diminishes and unreacted O remains on the surface (Fig. 4, S5, and S6). A small amount of $CO_2$ formation from the secondary combustion of the reaction intermediates is also detected. While the amount of ethanol reacting falls steadily, there is still some reactivity even up to the maximum O coverage studied, 0.75 Ml, indicating that ethanol is reactive even with densely packed oxygen or at defect structures therein.

## 4 Discussion

The linear dependence of the reactivity of methanol and ethanol with O and its 1:1 relationship between the ester formation and the O consumption, shows facile reaction between the alcohols and all the $O_{ads}$ within the zig-zag structure at low O coverage where the oxygen is highly dispersed (<0.08 Ml). Specifically, previous work showed that most oxygen atoms are composed of zig-zag chains which are 3–7 atoms long (Fig. 1c). Over this range of oxygen coverage, there is no difference between the overall reactivity of ethanol and methanol. These results indicate that the highest reactivity occurs when there is a substantial fraction of the O at the ends of the zig-zag chains and condensation of the chains into the 2D islands is minimal. Methanol reacts only at these very low coverages, suggesting that O at the chain ends is most reactive.

Because the alcohols were adsorbed in excess at 130 K and since the ester products evolve from the surface below 250 K, the reaction to form the adsorbed alkoxy as well as the subsequent reactions to form the esters must occur below 250 K, with the adsorbed O in its initial configuration, though its coverage is reduced as the reactions proceed. At O coverages above 0.08 Ml, methanol reactivity plateaus and then diminishes. As the zig-zag structure continues to develop toward saturation coverage at 0.25 Ml, the double row structure begins to form. In this regime (O coverage between 0.11 and 0.19 Ml) the density and length of the zig-zag structures increases, and defect regions, possibly due to local strain effects, appear (Fig. 1b). Methanol is clearly less reactive with O in this coverage region as the stability of the adsorbed O increases. Between 0.25 and 0.50 Ml, the double row structure develops and approaches saturation.

Ethanol, however, continues to react facilely (and linearly) with O between 0.08 and 0.35 Ml O, but over this range of coverage two oxygen atoms are consumed per ethyl acetate formed, clearly showing the participation of adsorbed O in the beta-C–H elimination steps. This behavior suggests that ethanol reacts readily with O in the zig-zag structure. While it is less reactive and certainly less selective for ester formation, it also clearly reacts with the double row O structure. Evidence for ethanol reaction with the double row structure is derived from the sustained, albeit reduced, reactivity of ethanol above 0.35 Ml of O—declining slightly at first and precipitously at 0.50 Ml O. In this range of higher O coverage some combustion begins, but much of the preadsorbed O simply remains unreacted.

One explanation of the lower reactivity of methanol versus ethanol in these studies is that the reactivity of methanol is limited by competitive desorption versus reaction. It is clear from the coincidence in the desorption of molecular methanol and production of methyl formate (Fig. 3) that molecular methanol is coadsorbed with the pre-adsorbed O at the dosing temperature throughout the range of O coverages studied, because reaction products were observed even above 0.50 Ml O. Furthermore, sites unoccupied by $O_{ads}$ are readily occupied by molecular methanol adsorption up to 0.50 Ml O. In order to test if desorption and reaction of methanol are competitive processes, temperature programmed reaction experiments were performed with heating rates varied over an order of magnitude. No difference was observed (Fig. S8). Hence, it must be concluded that the difference in the behavior between ethanol and methanol is due to inherently differing reactivity of the $O_{ads}$, which changes near 0.08 Ml O.

Another possible explanation for the difference in reactivity is that the thermodynamic driving force is different for formation of methoxy vs. ethoxy. Both the strength of bonding of the respective alkoxides and the heterolytic bond energies for the two alcohols differ. On clean Au(110) ethoxy is more strongly bound than methoxy by 2.3 kcal/mol [34]. This difference is due to larger van der Waals interactions of the ethoxy chain with the surface. Further, the energy required for deprotonation of methanol is 3.0 kcal/mol greater than that for ethanol [35]. Thus, the overall driving force for the acid-base reaction between methanol and adsorbed O is approximately 5 kcal/mol higher than that of ethanol. Even a small change in the energetics of the adsorbed O could thus lead to a dramatic change in reactivity between the two alcohols. Since oxygen atoms on the interior of the ordered O phases are more

stable than O at chain ends or present as monomers, the dispersed O at low coverage is more reactive, and both alcohols can react.

The most obvious change in the oxygen structure between 0.08 and 0.11 Ml O is the coalescence of the zig-zag chains into a more developed islands (Fig. 1). This structural progression leads to a broad maximum in the number of chain ends with increasing coverage, but the reactivity of methanol with $O_{ads}$ cannot be attributed to O only at the end of chains, because even at 0.06 Ml O all of the oxygen is reacted away (Fig. 1). The very existence of the chains and their aggregation into separated islands is suggestive of strain induced into the underlying surface. The abrupt change in reactivity of the methanol appears correlated to the creation of this strained oxygen overlayer, and that the strain either renders the $O_{ads}$ less reactive with methanol, or sufficiently reduces the strength of bonding of the alkoxy to the surface to render its formation energetically unfavorable. It is possible that this is a kinetic effect, realized through the different energetics of the transition states for the reactions of methanol and ethanol.

## 5 Conclusions

While it strongly correlates with the structure of the oxygen, the reactivity of methanol and ethanol for self-coupling is significantly different as a function of O coverage and structure. At low O coverage, where the O atoms are well dispersed in short chains, both alcohols behave similarly; 100% selectivity to the corresponding ester (methyl formate and ethyl acetate) is observed. Further, one ester is formed per preadsorbed O, indicating that the CH bond activation in the subsequent steps necessary to form the ester is facilitated by the gold surface itself. This deduction is further supported by the formation of sizeable amount of $D_2$ from isotopically labelled alcohols, which appears concomitantly with the ester. As the adsorbed O begins to coalesce into islands (above 0.08 Ml) O the alcohols react differently. The reactivity of the O with methanol decreases abruptly, whereas the additional O is recruited to activate β-D bonds in the ethoxy and perhaps the hemiacetal alcoholate as well. We attribute the differences in the reactivity of the two alcohols at the different O coverages to both strain in the O overlayer and differences in the overall energy of reaction of the abstraction of the alcoholic protons in methanol and ethanol.

**Acknowledgements** This work was supported as part of the Integrated Mesoscale Architectures for Sustainable Catalysis (IMASC), an Energy Frontier Research Center funded by the U.S. Department of Energy (DOE), Office of Science, Basic Energy Sciences (BES), under Award Number DE-SC0012573.

## References

1. Leibsle FM, Murray PW, Francis SM et al (1993) One-dimensional reactivity in catalysis studied with the scanning tunneling microscope. Nature 363:706–709. doi: 10.1038/363706a0
2. Zheng G, Altman EI (2002) The reactivity of surface oxygen phases on Pd(100) toward reduction by CO. J Phys Chem B 106:1048–1057. doi: 10.1021/jp013395x
3. Min BK, Alemozafar AR, Pinnaduwage D et al (2006) Efficient CO oxidation at low temperature on Au(111). J Phys Chem B 110:19833–19838. doi: 10.1021/jp0616213
4. Outka DA, Madix RJ (1987) The oxidation of carbon monoxide on the Au (110) surface. Surf Sci Lett 179:351–360. doi: 10.1016/0167-2584(87)90267-2
5. Gland JL, Kollin EB (1983) Carbon monoxide oxidation on the Pt (111) surface: temperature programmed reaction of coadsorbed atomic oxygen and carbon monoxide. J Chem Phys 78:963–974. doi: 10.1063/1.444801
6. Crew WW, Madix RJ (1996) A scanning tunneling microscopy study of the oxidation of CO on Cu(110) at 400 K: site specificity and reaction kinetics. Surf Sci 349:275–293. doi: 10.1016/0039-6028(96)80026-4
7. Gerrard AL, Weaver JF (2005) Kinetics of CO oxidation on high-concentration phases of atomic oxygen on Pt (111). J Chem Phys 123:224703–224703. doi: 10.1063/1.2126667
8. Min BK, Friend CM (2007) Heterogeneous gold-based catalysis for green chemistry: low-temperature CO oxidation and propene oxidation. Chem Rev 107:2709–2724. doi: 10.1021/cr050954d
9. Coulman DJ, Wintterlin J, Behm RJ, Ertl G (1990) Novel mechanism for the formation of chemisorption phases: The (2 × 1) O-Cu (110) added row reconstruction. Phys Rev Lett 64:1761–1766. doi: 10.1103/physrevlett.64.1761
10. Crew WW, Madix RJ (1994) Monitoring surface reactions with scanning tunneling microscopy: CO oxidation on p (2 × 1)-O pre-covered Cu (110) at 400 K. Surf Sci 319:L34–L40. doi: 10.1016/0039-6028(94)90587-8
11. Davies PR, Bowker M (2010) On the nature of the active site in catalysis: the reactivity of surface oxygen on Cu (110). Catal Today 154:31–37. doi: 10.1016/j.cattod.2009.12.011
12. Hashizume T, Taniguchi M, Motai K et al (1991) Field ion-scanning tunneling microscopy study of the Ag(110)-O System. Jpn J Appl Phys 30:L1529–L1531. doi: 10.1143/jjap.30.l1529
13. Pai WW, Reutt-Robey JE (1996) Formation of (n × 1)-O/Ag(110) overlayers and the role of step-edge atoms. Phys Rev B 53:15997–16005. doi: 10.1103/physrevb.53.15997
14. Taniguchi M, Tanaka K, Hashizume T, Sakurai T (1992) Ordering of Ag-O chains on the Ag (110) surface. Surf Sci Lett 262:L123–L128. doi: 10.1016/0039-6028(92)90120-U
15. Nakagoe O, Watanabe K, Takagi N, Matsumoto Y (2005) In situ observation of CO oxidation on Ag(110)(2 × 1)-O by scanning tunneling microscopy: structural fluctuation and catalytic activity. J Phys Chem B 109:14536–14543. doi: 10.1021/jp0512154
16. McEwan L, Julius M, Roberts S, Fletcher J (2010) A review of the use of gold catalysts in selective hydrogenation reactions. Gold Bull 43:298–306. doi: 10.1007/BF03214999
17. Hiebel F, Montemore MM, Kaxiras E, Friend CM (2016) Direct visualization of quasi-ordered oxygen chain structures on Au(110)-(1 × 2). Surf Sci 650:5–10. doi: 10.1016/j.susc.2015.09.018
18. Landmann M, Rauls E, Schmidt WG (2009) Chainlike Au-O structures on Au(110)-(1 × r) surfaces calculated from first principles. J Phys Chem C 113:5690–5699. doi: 10.1021/jp810581s
19. Xu B, Madix RJ, Friend CM (2014) Predicting gold-mediated catalytic oxidative-coupling reactions from single crystal studies. Acc Chem Res 47:761–772. doi: 10.1021/ar4002476

20. Pan M, Gong J, Dong G, Mullins CB (2014) Model studies with gold: a versatile oxidation and hydrogenation catalyst. Acc Chem Res 47:750–760. doi: 10.1021/ar400172u
21. Liu X, Xu B, Haubrich J et al (2009) Surface-mediated self-coupling of ethanol on gold. J Am Chem Soc 131:5757–5759. doi: 10.1021/ja900822r
22. Xu B, Liu X, Haubrich J et al (2009) Selectivity control in gold-mediated esterification of methanol. Angew Chem Int Ed 48:4206–4209. doi: 10.1002/anie.200805404
23. Xu B, Friend CM (2011) Oxidative coupling of alcohols on gold: insights from experiments and theory. Faraday Discuss 152:307–320. doi: 10.1039/c1fd00015b
24. Gong J, Flaherty DW, Yan T, Mullins CB (2008) Selective oxidation of propanol on Au(111): mechanistic insights into aerobic oxidation of alcohols. Chem Phys Chem 9:2461–2466. doi: 10.1002/cphc.200800680
25. Dhanak VR, Prince KC, Rosei R et al (1994) STM study of oxygen on Rh(110). Phys Rev B 49:5585–5596. doi: 10.1103/physrevb.49.5585
26. Africh C, Esch F, Comelli G, Rosei R (2002) Reactivity and deconstruction of the (1 × 2)-Rh (110) surface studied by scanning tunneling microscopy. J Chem Phys 116:7200–7206. doi: 10.1063/1.1465411
27. Africh C, Kohler L, Esch F, Corso M (2009) Effects of lattice expansion on the reactivity of a one-dimensional oxide. J Am Chem Soc 131:3253–3259. doi: 10.1021/ja808100f
28. Jensen F, Besenbacher F, Lægsgaard E, Stensgaard I (1990) Surface reconstruction of Cu(110) induced by oxygen chemisorption. Phys Rev B 41:10233–10239. doi: 10.1103/physrevb.41.10233
29. Personick ML, Madix RJ, Friend CM (2017) Selective oxygen-assisted reactions of alcohols and amines catalyzed by metallic gold: paradigms for the design of catalytic processes. ACS Catal 7:965–985. doi: 10.1021/acscatal.6b02693
30. Gong J, Flaherty DW, Ojifinni RA et al (2008) Surface chemistry of methanol on clean and atomic oxygen pre-covered Au(111). J Phys Chem C 112:5501–5509. doi: 10.1021/jp0763735
31. Outka DA, Madix RJ (1987) Broensted basicity of atomic oxygen on the gold (110) surface: reactions with methanol, acetylene, water, and ethylene. J Am Chem Soc 109:1708–1714. doi: 10.1021/ja00240a018
32. Xu B, Haubrich J, Baker TA, Kaxiras E (2011) Theoretical study of O-assisted selective coupling of methanol on Au (111). J Phys Chem C 115:3703–3708. doi: 10.1021/jp110835w
33. Xu B, Liu X, Haubrich J, Friend CM (2010) Vapour-phase gold-surface-mediated coupling of aldehydes with methanol. Nat Chem 2:61–65. doi: 10.1038/nchem.467
34. Karakalos S, Xu Y, Kabeer FC et al (2016) Noncovalent bonding controls selectivity in heterogeneous catalysis: coupling reactions on gold. J Am Chem Soc 138:15243–15251. doi: 10.1021/jacs.6b09450
35. Moylan CR, Brauman JI (1984) Bond dissociation energies in alcohols: kinetic and photochemical evidence regarding ion thermochemistry. J Phys Chem 88:3175–3176. doi: 10.1021/j150659a006